Cell Research (2012) 22:413-424.

www.nature.com/cr

ORIGINAL ARTICLE

Isolation and proteomic analysis of the SYP61 compartment reveal its role in exocytic trafficking in *Arabidopsis*

Georgia Drakakaki[1, 6], Wilhelmina van de Ven[1], Songqin Pan[1], Yansong Miao[2, 7], Junqi Wang[2], Nana F Keinath[3], Brent Weatherly[4, 5], Liwen Jiang[2], Karin Schumacher[3], Glenn Hicks[1], Natasha Raikhel[1]

[1]Department of Botany and Plant Sciences, Center for Plant Cell Biology, Institute for Integrative Genome Biology, 4119C Genomics Building, University of California Riverside, CA 92521, USA; [2]School of Life Sciences, Center for Cell and Developmental Biology, Chinese University of Hong Kong, New Territories, Hong Kong, China; [3]Heidelberg Institute for Plant Science, Im Neuenheimer Feld 230, Heidelberg 69120, Germany; [4]Complex Carbohydrate Research Center, University of Georgia, Athens, GA 30602, USA; [5]NuSep Inc., Bogart, GA 30622, USA

The endomembrane system is a complex and dynamic intracellular trafficking network. It is very challenging to track individual vesicles and their cargos in real time; however, affinity purification allows vesicles to be isolated in their natural state so that their constituent proteins can be identified. Pioneering this approach in plants, we isolated the SYP61 *trans*-Golgi network compartment and carried out a comprehensive proteomic analysis of its contents with only minimal interference from other organelles. The proteome of SYP61 revealed the association of proteins of unknown function that have previously not been ascribed to this compartment. We identified a complete SYP61 SNARE complex, including regulatory proteins and validated the proteome data by showing that several of these proteins associated with SYP61 *in planta*. We further identified the SYP121-complex and cellulose synthases, suggesting that SYP61 plays a role in the exocytic trafficking and the transport of cell wall components to the plasma membrane. The presence of proteins of unknown function in the SYP61 proteome including ECHIDNA offers the opportunity to identify novel trafficking components and cargos. The affinity purification of plant vesicles in their natural state provides a basis for further analysis and dissection of complex endomembrane networks. The approach is widely applicable and can afford the study of several vesicle populations in plants, which can be compared with the SYP61 vesicle proteome.

***Keywords*:** SYP61; *trans*-Golgi network; SNARE; proteomics; vesicles

Cell Research (2012) **22**:413-424. doi:10.1038/cr.2011.129; published online 9 August 2011, corrected publication 2023

Introduction

Plant growth and development are dependent on vesicular trafficking in the endomembrane system, which helps to package and deliver molecules to specific target destinations within the cell in response to internal and external signals [1]. The endomembrane system has many compartments, and a plethora of proteins, with roles in vesicular trafficking. However, pinpointing their precise functions is tremendously challenging because different compartments have similar or overlapping physicochemical properties. In addition, the nature of vesicular trafficking makes it difficult to distinguish between resident proteins with important functions in specific compartments and proteins that are carried passively between compartments as cargo. The high turnover rate of membrane proteins and the existence of multiple transport routes add to this complexity [1].

Exocytic vesicles are derived from the *tran*s-Golgi network (TGN) and are sent to the plasma membrane (PM), but the trafficking mechanism is poorly understood [2]. Golgi and post-Golgi trafficking has an essential role in cell wall biosynthesis and the delivery of transmem-

Correspondence: Natasha Raikhel
E-mail: nraikhel@ucr.edu
[6]Current address: Department of Plant Sciences, University of California, Davis, CA 95616, USA
[7]Current address: Department of Molecular and Cell Biology, University of California, Berkeley, CA 94720, USA
Received 31 December 2010; revised 1 April 2011; accepted 7 June 2011; published online 9 August 2011

brane receptors, cell wall enzymes, t-SNAREs and other membrane proteins to the PM [2]. In stark contrast to the mammalian endomembrane system, little is known about endocytic trafficking in plants [3, 4]. Endocytic trafficking of plant PM proteins involves either recycling or degradation as required, the latter involving vesicular transport to the vacuole [3, 4]. The TGN is considered an early endosome (EE) compartment because it is rapidly labeled with the endocytic marker FM4-64 [5]. It is implicated in endocytic, secretory trafficking and retromer-mediated recycling of vacuolar sorting receptors (VSRs) [6, 7].

Vesicle isolation is the most direct method of dissecting the role of TGN vesicles in their natural state, in which their constituent proteins can be identified. Proteomes of cytoplasm [8], endoplasmic reticulum (ER) and PM [9], and several organelles, including Golgi [9], vacuole [10], mitochondria [11], peroxisomes [12] and chloroplast [13], have been isolated from plants; however, so far the isolation of vesicles has been an insurmountable challenge.

In mammalian cells, immunoisolation of vesicles has been performed, for example, from mouse brain cells [14] and has provided insights into trafficking pathways. However in plants, partially due to the strong interference of cell wall in extraction procedures, successful vesicle isolation has so far not been demonstrated.

Overcoming current technical limitations, we took advantage of the SNARE protein syntaxin of plants 61 (SYP61) to isolate TGN vesicles by affinity purification. SYP61 is a TGN-localized Q-SNARE and is part of a protein complex that includes VTI12 and SYP41 Q-SNAREs and other regulatory proteins such as VPS45 [15, 16]. The SYP61 compartment appears to function as an EE for specific PM proteins [17]. The exact role of SYP61 is unclear, but it has been implicated in stress responses induced by abscisic acid [18], and it may be involved in trafficking of components to and from the prevacuolar compartment (PVC) [6, 7, 15, 16, 19]. In order to clarify the role of SYP61, and characterize the compartment in which it resides in endomembrane trafficking, we purified SYP61 vesicles using a novel, universally adoptable immunoisolation procedure for plants and conducted a detailed proteomic analysis of the vesicle components. *In planta* subcellular localization of candidate proteins corroborated their localization within SYP61 vesicles.

Results and Discussion

Vesicle isolation and proteomic analysis

SYP61 vesicles were isolated from transgenic *Arabidopsis* plants expressing SYP61::SYP61-CFP, using a two-step procedure comprising sucrose-gradient fractionation, followed by immunopurification with antibodies against GFP. The fractionated sample was enriched for the SYP61 fusion protein, but contained minor traces of the abundant ER marker BiP [20] and the PVC marker SYP21 [21] (Supplementary information, Figure S1). These contaminants were eliminated in the second immunopurification step (Figure 1A). Transmission electron microscopy confirmed the integrity of the isolated vesicles (Figure 1Bi), and immunonegative staining verified the presence of SYP61 in the isolated vesicles (Figure 1Bii).

Vesicle proteins were digested with trypsin while attached to beads and analyzed by nano-liquid chromatography coupled to tandem mass spectrometry (nano-LC/MS/MS), resulting in the identification of multiple SYP61-specific peptides (Figure 1C, and Supplementary information, Table S2). A multidimensional protein identification technology (MudPIT) method with two-dimensional nano-ultra-performance liquid chromatography (UPLC) was used to analyze tryptic peptides derived from co-IP pull-down samples for three biological replicates, with IgG as a negative control. Mascot was used with *Arabidopsis* Tair 10 decoy database for protein identification. The Mascot output files were further analyzed with the ProteoIQ [22] software to determine positive protein identification at 1% false-discovery rate (FDR; see Materials and Methods). Comparison of proteins between SYP61 and IgG pull-down was made, and proteins detected at least in two of the three replicates in the SYP61 sample but not in IgG control were considered specific to SYP61 compartment (Supplementary information, Table S1) following the same criteria previously described in mouse vesicle isolation [14]. Despite the several steps of purification, minor traces of some abundant background proteins were present in the final proteome as previously observed by other proteomic studies [23]. A few proteins were detected with much higher sequence coverage/spectral counting (SC) in SYP61 pull-down than in IgG. These proteins were further quantified with the accurate mass and retention time (AMRT) method [24, 25] using MS spectra intensity derived from extracted

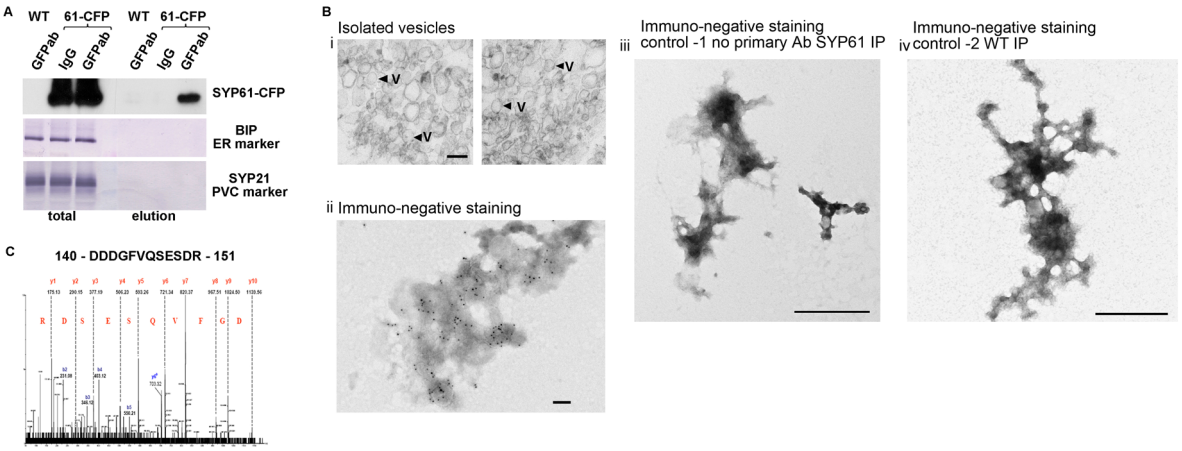

Figure 1 Immunoisolation of SYP61 vesicles. **(A)** Immunoblot analysis of the 33%–8% interface fraction of sucrose gradient of wild-type and SYP61::SYP61-CFP samples, before (total) and after immunoisolation (elution), using beads coupled with GFP antibodies (GFPabs) or beads coupled with IgG (IgG). Samples were incubated with antibodies against SYP61, BiP and SYP21. WT = Wild Type, Col-0. **(B)** (i) Transmission electron micrographs showing the ultrastructure of immunoisolated vesicles. (ii) Negative staining and immunolocalization of purified vesicles with the anti-SYP61 antibody. V, vesicle. Scale bar in (i, ii) = 100 nm. (iii) Negative control for ii, immunoisolated compartments from SYP61::SYP61-CFP samples followed by labeling without the presence of primary antibody. (iv) Negative control for ii, immunoisolated compartments from WT plants, followed by labeling with anti- SYP61 antibody. Scale bar in (iii, iv) = 500 nm. **(C)** A representative peptide nano-LC/MS/MS spectrum of SYP61 found in the immunoisolated vesicles.

ion chromatogram (XIC) of continuum LC/MS scans to include only statistically significant proteins (see Material and Methods, Supplementary information, Table S2 columns X and Y and Figure S2).

Together, we identified 145 proteins that were specific in the SYP61 immunoisolated fraction compared to the IgG control.

We observed that neither SYP21 nor SYP51 [16], which are known PVC markers, was identified in the SYP61 proteome, demonstrating that using this approach we can separate endomembrane vesicles that are very similar in size and are difficult to separate by density gradients [26]. Proteins with significant scores included integral membrane proteins, such as components of the SYP61-annotated SNARE complex (SYP41, VTI12) and their regulatory protein VPS45 [16, 19], the vacuolar proton pump subunit VHA-a1 [5] and proteins transiently associated with vesicles, such as the *N*-ethylamide-sensitive factor.

The SYP61 vesicle proteome contained many proteins known to be involved in vesicle trafficking, such as GTPases and proteins involved in TGN and endosome sorting, as well as enzymes such as pectin methylesterase and hydrolases, that could represent cargo (Supplementary information, Tables S1 and S2). Several of these proteins are known to be located in the PM, including cellulose synthases and SNAREs such as SYP121 and VAMP72. Overall, 60% of the identified proteins are known or predicted to be associated with the endomembrane system, and 8% currently have no assigned function (Supplementary information, Tables S1 and S2). The rest of the proteins represent cargo being transported by SYP61 vesicles. When our data were compared with the previously annotated Golgi proteome [9], we found 11 proteins common in both analysis. Several proteins are involved in carbohydrate biosynthesis including members of the cellulose synthase superfamily, such as components of cellulose synthase A1 (CESA1) and CESA3, which traffic from Golgi to the PM [27]. These data indicate that the Golgi proteome does not include the population of TGN vesicles and validate the specificity of our approach separating the SYP61 vesicles from Golgi. Moreover, proteins that were not classified by LOPIT [9] were identified in the SYP61 vesicle proteome.

The SYP61 proteome includes a complete SNARE complex and its regulatory proteins

During vesicle fusion, syntaxins recognize and assemble in complexes with two other SNARE proteins on the target membrane, forming a three-helix bundle (t-SNARE complex), which interacts with a fourth SNARE on the vesicle membrane [28]. The SYP61 proteome included two Qa-SNARE proteins (SYP41 and SYP43), one Qb protein (VTI12), the bait Qc protein SYP61 and the regulatory protein VPS45. Immunocytochemical experiments with protoplasts isolated from SYP61-CFP transgenic plants confirmed the localization of VPS45 (Supplementary information, Figure S3A-S3C) and corroborate with previous reports describing a SYP41/SYP61/VTI12 SNARE complex [16, 19, 29]. Other SYP4 members such as SYP43 were also found in the SYP61 vesicle proteome, establishing new protein association with SYP61. Colocalization with SYP61-CFP in stably transformed plants (Supplementary information, Figure S3D-S3F) further indicates a novel interaction within the SYP61 SNARE complex.

In summary, a complete SNARE complex, including its regulatory proteins, was identified in SYP61 vesicles, confirming the sensitivity of our approach, the purity of the vesicles and its ability to detect novel protein interactions.

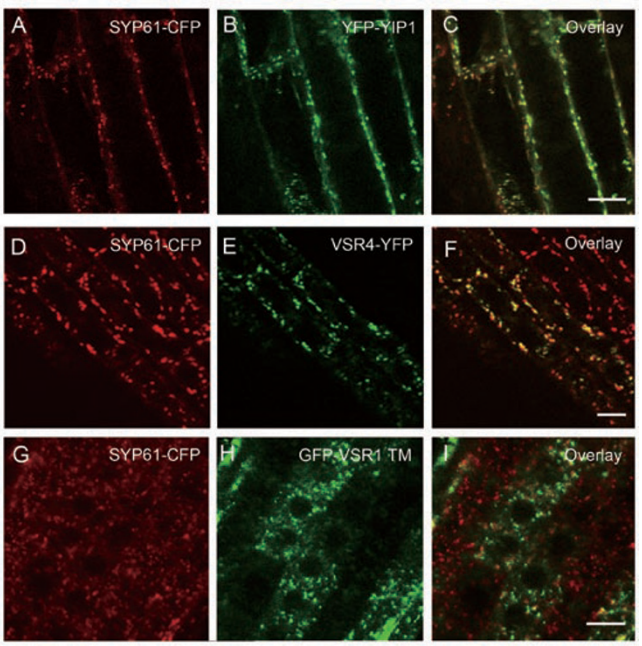

Figure 2 SYP61 colocalization with YIP and VSRs. **(A-C)** Colocalization of SYP61::SYP61-CFP (red) and 35S:YFP-YIP (green) in *Arabidopsis* root cells. **(D-I)** SYP61 colocalizes with VSR4 and partially colocalizes with VSR1. Confocal images of SYP61::SYP61-CFP (red) and 35S::VSR4-YFP and 35S::GFP-VSR1TM (green). Scale bar = 10 μm.

Vesicle tethering components of the SYP61 compartment

A variety of proteins with a role in membrane trafficking were identified in the isolated SYP61 compartment, including YIP1. In yeast, Yip1p was initially isolated in a screen for proteins that interact with the transport GTPases Ypt1p and Ypt31p. Yip1p recruits these proteins specifically to Golgi membranes, an expected function for the GTPase receptors. It is predominantly located at the Golgi membranes, but when expressed at high levels it can also be found in the ER [30]. The mammalian homologs (Yip1 and Yip1A) are found in the Golgi and at ER exit sites [31]. Recent studies show that Yip1A regulates the membrane association of Rab6, indicating a role in the Golgi or TGN [32]. There are seven *Arabidopsis* YIPs, two of which were identified in the SYP61 proteome (Supplementary information, Table S1). We selected (At3g05280) YIP1 for colocalization experiments and observed that the YFP-YIP1 fusion protein colocalized with SYP61-CFP in stably transformed plants, supporting a role in the TGN (Figure 2A-2C).

GTPases were abundantly present in the SYP61 proteome (Supplementary information, Tables S1 and S2) including RABD2a and RABD2b, which have been shown to colocalize in the Golgi and TGN [33, 34]. Likewise, we showed that RABD2b and SYP61 colocalized in *Arabidopsis* plants (Supplementary information, Figure S3G-S3I). Mammalian Rab1 and its yeast homolog Ypt1p interact with similar effector proteins, promoting the targeting of COPII vesicles to the *cis*-Golgi [35]. Unlike mammalian Rab1, our data allow us to put forward the hypothesis that the RABD2 GTPase is recruited by YIP1 to the SYP61 compartment at the TGN.

During vesicle fusion, tethering factors, such as the transport protein particle (TRAPPI and TRAPPII) complexes, function upstream of SNAREs, acting over long distances to bring the interacting complexes together and to provide additional compartment specificity [36]. The SYP61 proteome contained a Trs120 homolog, a member of the TRAPPII complex with a putative role in cytokinesis [37]. It included four orthologs of TRAPPI complex subunits (At5g54750, At5g58030 and At3g05000 as potential Bet3 subunits, and At5g16280 as potential Trs85 subunit). TRAPPI is involved in ER to Golgi transport in yeast and functions as a guanine nucleotide exchange factor for the early acting Rab1 homolog Ypt1 [38]. The identification of multiple components of the TRAPPI complexes in SYP61 vesicles suggests that plant TRAPPI might be involved in vesicle fusion at the TGN rather than ER to Golgi transport.

VSRs in the SYP61 compartment

In the plant endomembrane system, the classic trafficking model involves two types of cargo-carrying signals that direct proteins to the vacuole via different routes, either *N*-terminal sorting signals (ntVSS) [39] or *C*-terminal sorting signals (ctVSS) [40]. *Arabidopsis* has seven VSR homologs (AtVSR1-AtVSR7), and thus far the functions of VSR1, VSR3 and VSR4 have been mainly investigated using genetic approaches [29, 41, 42]. However, little is known about the trafficking of VSRs through the SYP61 compartment. VSR1 is thought to direct ntVSS cargo to the PVC in a clathrin-dependent pathway [43], although recent studies have expanded this view by showing that ctVSS cargo follows the same route [41, 44, 45]. Our proteomic analysis revealed the presence of several VSRs in SYP61 vesicles, including VSR4 (At2g14720), VSR3 (At2g14740) and VSR7 (At4g20110; Supplementary information, Tables S1 and S2), with localization studies showing clearly that VSR4-YFP was colocalized with SYP61-CFP in stably transformed plants (Figure 2D-2F).

VSR1TM is a derivative of VSR1, containing the signal peptide, the transmembrane domain and the cytoplasmic tail [46]. A GFP-VSR1TM fusion [46] was partially colocalized with SYP61 (Figure 2G-2I) as was VSR2-YFP (Supplementary information, Figure S4A-S4C). The partial localization supports participation of VSRs 1, 2 and 3 in different trafficking routes in comparison to VSR4 in *Arabidopsis*. VSR1, 2 and 3 recycle in SYP61 from PVC [47], while VSR4 might be involved in an independent trafficking route. Different results regarding the localization of VSR4 have been presented recently in transgenic tobacco [48] or *Arabidopsis* [49] showing either late PVC or punctate and PM localization of VSR4. Our data corroborate with the later studies suggesting that VSR4 also follows a SYP61 pathway to the PM and recycles back to EE.

SYP61 facilitates the trafficking of proteins to the PM

SNARE proteins are structurally classified into Q and R groups [50] or functionally specified as vesicle-associated (v-) or target-associated (t-) SNAREs. Homotypic fusion and anterograde traffic add complexity to the latter classification. SYP61 has thus far been considered solely as a TGN resident, with no involvement in anterograde transport to the PM. It has been shown that the SYP121 Qa-SNARE PM resident (PEN1) [51] interacts with the SNAP33 adaptor and the two functionally redundant VAMP72 synaptobrevins [52] in forming the PEN1-SNAP33-VAMP721/VAMP722 tertiary SNARE complex that contributes to a fungal resistance system [52, 53]. In the leaf epidermis, VAMP722-GFP vesicles

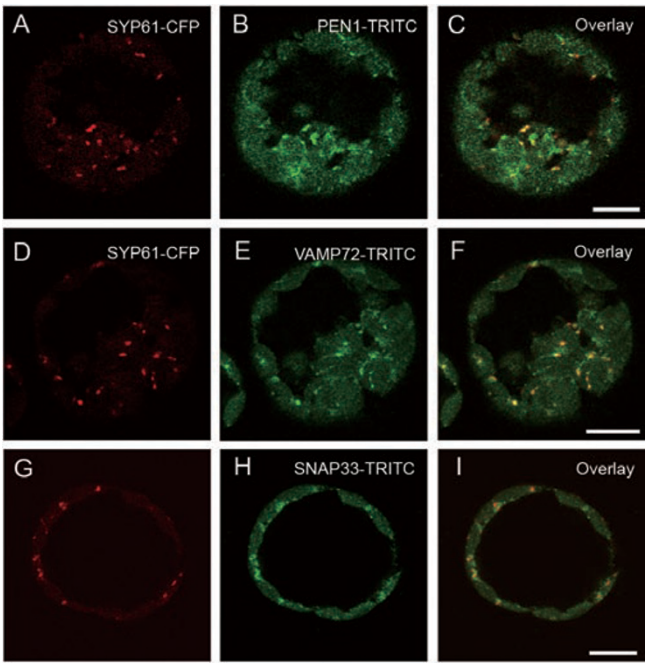

Figure 3 Colocalization of SYP61 with the SYP121 complex. **(A-C)** Colocalization of SYP61 (red) with PEN1-FITC (green); **(D-F)** VAMP72-FITC; and **(G-I)** SNAP33-FITC in *Arabidopsis* SYP61::SYP61-CFP protoplasts. Scale bar = 10 μm.

accumulate in intracellular compartments in response to an infection by *Blumeria graminis*. They accumulate directly beneath the appressoria [52], inducing pathogen focal secretion as a disease resistance mechanism. In the SYP61 proteome, SYP121 and VAMP722 were detected, and SYP121, VAMP722 and SNAP33 were shown to be colocalized with SYP61-CFP (Figure 3). This points to a potential SYP61 involvement in the trafficking mechanisms of the SYP121 complex induced by pathogens. A general role in stress adaptation is implied by the association between SYP61 and drought responses [18], and between SYP121 and adaptations to several forms of abiotic stress [54]. Kwon *et al*. [52] propose that SYP121 facilitates the secretion of cell wall components to the PM in response to pathogen attack. The cumulative data in this study highlight that SYP61 is likely to be involved in the same process.

Several CESA complexes were identified in the SYP61 proteome (Supplementary information, Table S1), therefore colocalization experiments were performed with all the available components of the complex that are involved in primary cell wall biosynthesis, i.e., CESA1 (Supplementary information, Figure S5), and CESA6 and CESA3 [55-57]. Overlapping fluorescence signals were observed between SYP61-CFP and each of the compo-

nents tested; hence, a more detailed analysis was carried out by EM immunostaining (Figure 4). Single labeling of SYP61 confirmed its localization in vesicles of the TGN and in close proximity to the PM (Figure 4A, 4B and 4D). The same results were observed in SYP61/CESA6-YFP double-labeling experiments, confirming the role of SYP61 in the trafficking of CESA complexes to the PM. The analysis was extended to plants treated with endosidin 1 (ES1), a specific inhibitor of SYP61 trafficking [17], revealing that SYP61 and CESA6-YFP colocalize in ES1 bodies (Figure 4C). This clearly demonstrates that CESA trafficking is TGN dependent.

The SYP61 proteome also contains a putative secretory carrier membrane protein (At1g61250, SCAMP1), which colocalizes with SYP61-CFP in TGN vesicles and in the PM as shown with two independent methods, YFP fusion to SCAMP and immunocytochemistry (Figure 4G-4I and Supplementary information, Figure S6). YFP fusions of plant SCAMPs have been localized to many endomembrane compartments, including EE, PM, secretory vesicles and the cell plate [58, 59]. Moreover, ES1 treatment showed that trafficking of SCAMP1 in *Arabidopsis* is TGN dependent (Figure 4F), validating its colocalization with SYP61 in TGN vesicles.

The involvement of SYP61 in trafficking of cell wall components and disease resistance complex could indicate that a vesicular transport mechanism can be induced under biotic and abiotic stress conditions.

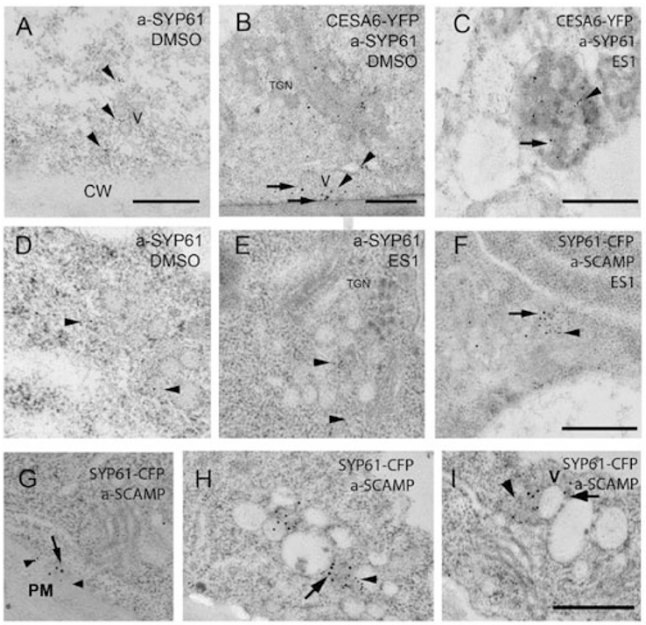

Figure 4 ImmunoEM localization of SYP61 with CESA6-YFP in untreated and ES1-treated *Arabidopsis* plants subjected to high-pressure frozen/freeze substitution. **(A**, **B**, **D**) ImmunoEM localization of SYP61 in vesicles and in the PM with CESA6-YFP in DMSO treated seedlings. **(C**, **E)** Localization and colocalization of SYP61 (10 nm) with CESA6-YFP (15 nm) in ES1 bodies. Arrowheads indicate SYP61 labeling. Arrows indicate CESA6-YFP labeling. **A**-**C** represents hypocotyl tissues; **D** and **E** represent root tissue. **(F-I)** Immunocytochemical analysis of ultrathin sections of roots stained with anti-GFP (15 nm) and anti-SCAMP1 (10 nm) by immunogold labeling showing colocalization of SYP61::SYP61-CFP and SCAMP in the PM and in vesicles. ES1-treated seedling is shown in **F**. Arrows indicate SCAMP1 labeled with gold particles. Arrowheads indicate SYP61 labeled with gold particles. PM, plasma membrane; V, vesicle; TGN, *trans*-Golgi network. Scale bar = 500 nm.

The SYP61 vesicle proteome contains many proteins with unknown function

The identified SYP61 vesicle proteome contained a number of annotated proteins and this association has provided extensive data concerning the role of the SYP61 pathway and its interaction with other pathways. However, several uncharacterized proteins were also detected in the SYP61 proteome, providing the first indications of their functions (Supplementary information, Tables S1 and S2). Two of these proteins, AT1G09330 (proposed name: ECHIDNA [60]) and AT2G45010), were selected for further colocalization experiments, on the basis of their relatively high score. In both cases, the signals for cognate YFP fusion proteins overlapped with SYP61-CFP in stably transformed plants (Figure 5A-5C, 5J-5L).

AT1G09330-YFP formed punctate structures that were sensitive to brefeldin A (BFA) [61] and ES1 [17], and predominantly colocalized with SYP61-CFP (Figure 5D-5I). TVP23p, the yeast homolog of AT1G09330, is localized to late Golgi compartments and interacts with Yip4 and Yip5 [62]. Since the SYP61 compartment also contains YIP1, we suggest that AT1G09330 (ECHIDNA) might colocalize and function together with proteins found in SYP61 vesicle proteome. YFP-AT2G45010 co-localized with SYP61-CFP in both endosomes and in the PM. BFA caused both the proteins to accumulate in BFA bodies (Figure 5G-5I, 5P-5R), confirming their shared use of a Golgi-dependent pathway. Both proteins were ES1 sensitive, accumulating in SYP61 ES1-induced bodies, indicating trafficking through the SYP61 compartment (Figure 5D-5F, 5M-5O).

Conclusions

The isolation of vesicles is a highly valuable strategy to dissect the complex and dynamic nature of the plant endomembrane system, but several difficulties such as

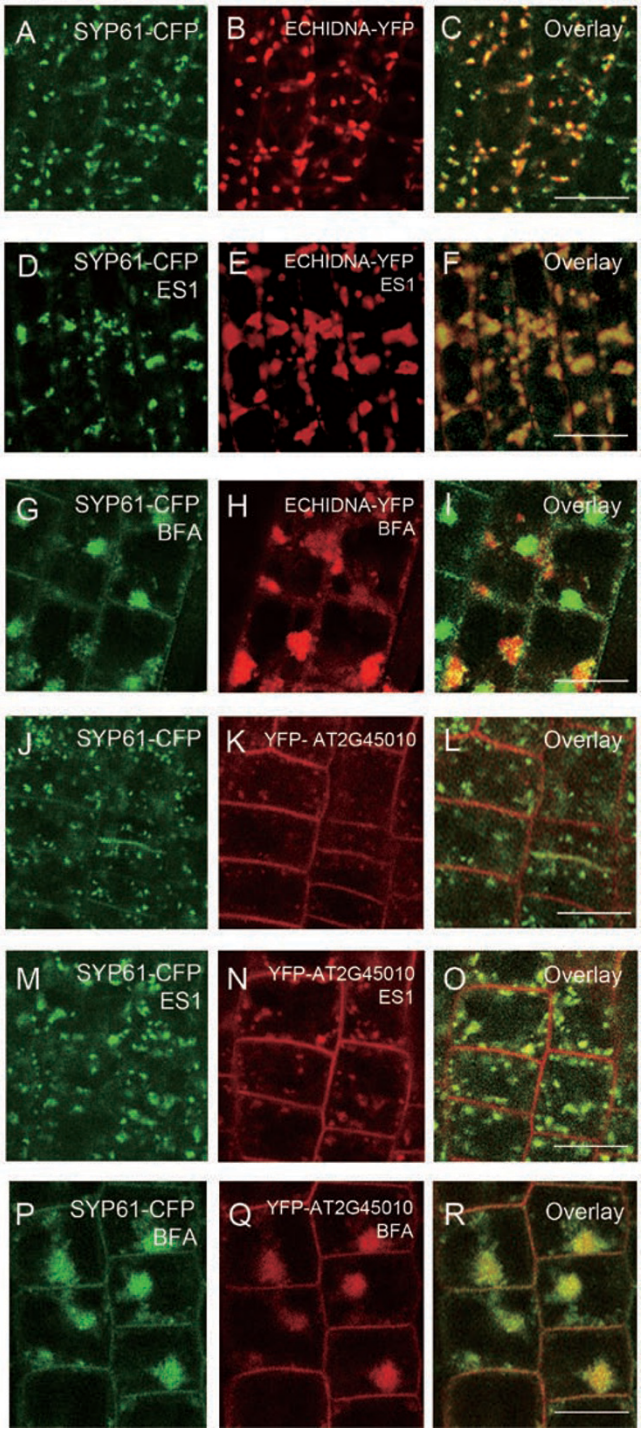

Figure 5 Subcellular localization of proteins with unknown function in *Arabidopsis*. **(A-I)** Colocalization of SYP61 and AT1G09330 (ECHIDNA) in stably transformed plants under different chemical treatments. **(A-C)** DMSO; **(D-F)** ES1; **(G-I)** BFA; **(A**, **D**, **G)** SYP61::SYP61-CFP; **(B**, **E**, **H)** 35S::AT1G09330-YFP; and **(C**, **F**, **I)** overlay. **(J-R)** Colocalization of SYP61 with AT2G45010 under different treatments. **(J-L)** DMSO; **(M-O)** ES1; **(P-R)** BFA; **(J**, **M**, **P)** SYP61::SYP61-CFP; **(K**, **N**, **Q)** 35S::YFP-AT2G45010; and **(L**, **O**, **R)** overlay. Scale bar = 10 μm.

separation from other vesicles have been a major impediment in its application. We developed an affinity-based vesicle isolation methodology for plants and successfully coupled it with proteomics to gain insights into the components and function of the SYP61 vesicle, and its relationship with other pathways. The quantitative proteomics approach allowed us to exclude non-vesicle proteins from the immunopurified vesicles. The specificity of candidate vesicle-specific proteins, both resident and cargo, was validated by colocalization analysis with fluorescent fusion proteins using confocal microscopy. The combination of immunoisolation and quantitative proteomics proved to be very efficient, as the identified candidate proteins were indeed colocalized with SYP61 in *Arabidopsis*.

A complete SNARE complex as well as several proteins involved in vesicle fusion, tethering and trafficking were part of the SYP61 proteome. This included a new member of the SYP4 family, whose presence demonstrates that several SYP4 proteins are used in the SYP61-SNARE complex, acting in different cells or at different developmental stages.

Several GTPases and YIPs were identified in the SYP61 proteome, showing that they can be located in the TGN in plants, which contrasts with their localization in yeast. This shows that despite their conserved functions, these proteins localize differently, indicating subtly different roles in trafficking. The identification of several VSRs in the SYP61 proteome revealed a subcellular specificity that may assist in the dissection of different trafficking pathways regulated by these proteins.

Isolated vesicles revealed the presence of cargo destined for the PM, including CESAs, highlighting the potential role that SYP61 vesicles play in secretion. CESAs are localized in distinct vesicles, known as microtubule-associated cellulose synthase compartments (MASCs) or small CESA compartments (SmaCCs) [56, 57]. SmaCCs partially colocalize with SYP61 [56, 57], whereas MASCs lack other endosomal markers and are thought to represent a new and independent compartment. In our investigation, the SYP61 compartments that colocalized with CESA6-YFP may therefore represent SmaCCs. It is tempting to speculate that SmaCCs originate from the TGN by a maturation mechanism [63] of SYP61 vesicles targeted to the PM. As a whole, the above data strongly support the hypothesis that SYP61 vesicles are involved in the trafficking of CESAs to the PM. These findings open the question whether SYP61 is a part of the SmaCC/MASC pathway or CESA endocytosis is facilitated by SYP61 vesicles. It is plausible that SYP61 vesicles are normally located at the TGN, with secretory activity being induced by stress as part of a defense/ad-

aptation mechanism. This suggests that CESA-containing vesicles may also carry the SYP121 complex.

The SYP61 proteome also contained several proteins with unknown functions, including AT1G09330 (ECHIDNA), and proteins not previously described as part of the SYP61 compartment. The presence of such proteins and their interactions with well-characterized proteins in the same compartment shed light on their functions and allow tentative annotations. The affinity purification of SYP61 vesicles combined with quantitative proteomics therefore provides a basis for the identification and characterization of proteins that currently have no assigned function and the cataloging of their interactions with other vesicle components. The SYP61 proteome can be compared with other organelle proteomes, specifically Golgi, and can provide insights on cellular compartmentalization. Adopting this approach several compartments can be isolated, which should provide an increased understanding of vesicle trafficking and the plant endomembrane system as a whole.

Materials and Methods

Plant material

Arabidopsis thaliana Col-0, wild-type plants and transgenic lines expressing SYP61-CFP [17], were grown in liquid MS medium for 14 days [64]. Golgi/TGN vesicles were isolated by gently grinding leaves in chilled vesicle isolation buffer (HEPES 50 mM, pH 7.5, 0.45 M sucrose, 5 mM MgCl2, 1 mM DTT, 0.5% PVP (P2307, Sigma) and protease inhibitors (Roche)) and by separating the Golgi/TGN as previously described [65].

Immunoprecipitation of SYP61 vesicle fraction

GFP antibody (A11122, Invitrogen) and normal rabbit IgG (sc-2027; Santa Cruz Biotechnology Inc.) were coupled to Protein A agarose beads (Invitrogen) for 3 h at 4 °C in phosphate-buffered saline and equilibrated in resuspension buffer (50 mm HEPES pH 7.5, 0.25 M Sucrose, 1.5 mM $MgCl_2$, 150 mM NaCl and protease inhibitors (Roche)). Plant vesicle extracts were pretreated with unconjugated beads for 20 min to remove nonspecific binding proteins and then incubated with the antibody-coated beads for 2 h at 4 °C to collect SYP61 vesicles. After two washes in resuspension buffer, the beads were washed in 1 ml 50 mM NH_4CO_3 (pH 8) and stored for proteomic analysis.

MudPIT nano-LC/MS/MS and nano-LC/MS analyses

Sample preparation was carried out as described in Supplementary information, Data S1. A Waters system of 2D nano-Acquity UPLC and Q-TOF premier tandem mass spectrometer was used for all proteomics experiments (Waters, Milford, MA). A combination of high-pH reverse phase and conventional low-pH reverse phase served as a MudPIT method following the manufacturer's recommendation (Waters). The solvents for the first-dimension LC of high-pH reverse phase were 20 mM ammonium formate, pH 10, (solvent A) and 100% acetonitrile (solvent B), respectively. The online fractionation was carried out with a trap column and percentage of solvent B. The peptide sample was loaded onto an XBridge BEH130 C18 trap column (8 µm particle, 300 µm i.d., 5 cm long, PN# 186003682; Waters). The partial-loop sample-loading method was configured with a 10 µl sample loop in the auto sampler for maximal loading with zero sample loss (6 µl for each experimental injection). The fractionation and desalting were carried out using a 2D-dilution method configured within the 2D nano-Acquity and controlled with MassLynx 4.1 (Waters). There were 10 fractions and 2 flushes based on percentage of solvent B as follows: (1) 8.2%; (2) 11.7%; (3) 13%; (4) 14.5%; (5) 15.9%; (6) 17.4%; (7) 18.9%; (8) 20.4%; (9) 23.6%; (10) 45%; (11) 65% (flush 1); and (12) 80% (flush 2). Mass spectrometry data were acquired for all of the 12 fractions.

For the second-dimension LC, a BEH130 C18 column (1.7 µm particle, 75 µm i.d., 20 cm long, PN# 186003544; Waters) was used for peptide separation. A Symmetry C18 (5 µm particle, 180 µm i.d., 20 mm long, PN# 186003514; Waters) served as a trap/guard column for desalting and pre-concentrating the peptides for each MudPIT fraction. The solvent components for peptide separation were as follows: mobile phase A was 0.2% formic acid in water, and mobile phase B was 0.2% formic acid in acetonitrile. The separation gradient was as follows: at 0 to 1 min, 0% B; at 3 min, 3% B; at 5 min, 8% B; at 70 min, 45% B; at 85 min, 60% B; at 95 min, 90% B; at 95 to 100 min, 90% B; at 105 min, 10% B; at 110 min, 0% B; and at 110 to 135 min, 0% B. The nano-flow rate was set at 0.3 µl/min without flow-splitting. A blank injection using the same LC method was introduced between each sample to remove carryovers or contaminants.

The parameters for the MS instrument were following: nano-ESI+ selected as ionization source using the Nano-sprayer (Waters) coupled with a PicoTips emitter (PN# FS360-20-10-CE-20, New Objective, Woburn, MA), capillary voltage set at 3 kV, sample cone voltage 42 V, extraction cone voltage 3.0 V, collision energy for MS1 scan 5 V, TOF reflectron operated in V-mode, source temperature set at 100 °C, MS resolution was 10 000 at FWHM for V-mode and MCP/TDC detector (micro-channel plate/time-to-digital converter) voltage set at 1 950 V. Mass accuracy was externally calibrated using a standard peptide such as GFP, and all MS measurements were within 123 ppm. Both LC and MS operation and data acquisition were controlled by the central software, MassLynx 4.1 (Waters).

Nano-LC/MS/MS was carried out for each fraction of the MudPIT experiment with a data-dependent acquisition (DDA) survey method, and data were acquired for run times between 15 and 115 min, with a MS1 *m/z* range from 350 to 1 900. MS1 scan time for precursor ions was 1 sec, with a 0.1 sec interscan delay. For each MS1 scan, a maximum of four ions were selected (whose individual peak intensity was above 30 counts/scan), for MS/MS scans with the collision-induced dissociation (CID) method to generate fragment spectrum. Individual MS/MS scans switched either when total ion current reached 2 000 counts or when the total scanning time exceeded 8 sec. Single MS/MS scan time was set for 1.9 sec, with a 0.1-sec interscan delay. A quadruple collision cell was used for CID fragmentation, and argon gas was chosen as collision gas with a flow rate of 0.45 ml/min. A charge state recognition file was used to determine the collision energy based on *m/z* values and charge states of each ion. The deisotoping method was employed to avoid repetitive scans for the same peptide ion, with the deisotoping window set to 3 Da. Real-time exclusion was enabled, with

the exclusion window set at 80 mDa for 10 min. Only ions with multiple charges were selected for MS/MS scan. For the same sample, a continuum LC/MS run was also carried out with identical parameters; however, the MS1 scan was never switched to MS/MS to completely accumulate all precursor ions for a label-free, AMRT quantitative analysis [24, 25]. All these experiments were controlled again by MassLynx4.1 (Waters).

For one of the three biological replicates, we also employed the "drill-down" approach to improve the detection of low-abundance peptides [66]. The exclusion window in the "drill-down" method was set at 60 mDa for *m/z* and 900 seconds for the retention time.

Protein identification and determination of vesicle-specific proteins

All the DDA data were processed by PLGS 2.2.5 (ProteinLynx Global Server, Waters) to generate peak lists for all MS/MS spectra in the pkl format using the following data enhancement: adaptive background subtraction, Savitzky-Golay peak smoothing using two iterations and three channels, fast deisotoping with a threshold of 3% and a minimum peak width of four channels, peaks centroided at 80% of their apical peak height, TOF resolution set to 10 000 and the NP multiplier set at 0.515.

Protein database search was carried out with the Mascot 2.3 search engine and the *Arabidopsi*s TAIR10 protein database supplemented with its reverse sequences, a common contaminant list (ftp://ftp.thegpm.org/fasta/cRAP/crap.fasta), antibody sequences and CFP-SYP61 fusion sequence. The Mascot search parameters were as follow: trypsin, auto-hit, 150 ppm for MS1, 0.3 Da for MS/MS, five variable modifications including acetyl (N-term), formyl (N-term), pyro-Glu (N-term E or Q) and oxidation (M). The database search was executed with Mascot Daemon. Individual pkl files were searched independently or they were merged on sample/replicate basis.

To identify putative SYP61-compartment proteins, the Mascot result files (.dat format) were further processed using the software package ProteoIQ ver 2.1 (NuSep Inc., Athens, GA, USA) to determine a validated protein list and to approximate the quantitative differences between the SYP61 and IgG samples based on identified peptides. The proteins were filtered using a 1% protein FDR using the ProValT algorithm [22] as implemented in ProteoIQ. The protein list was further filtered such that each protein was identified in at least two replicates of the SYP61 sample but not at all in the three IgG samples [14]. Proteins that were detected in both SYP61 and IgG were selected for further quantification analysis if their number of peptides detected in SYP61 was at least three times the number of peptides identified in IgG (Supplementary information, Table S2). As a default output of ProteoIQ, relative SC was also performed and displayed as Log_2(SYP61-SC/IgG-SC). Proteins with a spectral count of 0 in IgG were shown to have Log2 values of 10 in SYP61.

A label-free AMRT quantitative strategy [24, 25] was employed to further validate the specificity of those proteins that were also detected in IgG with few peptides. A representative peptide ion of each of these proteins was manually extracted from continuum nano-LC/MS XIC with the software MassLynx 4.1 based on its detected MudPIT fraction, *m/z*, charge state, and retention time. Then, all MS scans for each representative ion were summed across its retention time to obtain the total signal intensity (Supplementary information, Figure S2). The MS spectra signals were compared between SYP61 and IgG samples across the three biological replicates. Only proteins with a significant SYP61/IgG ratio ($P < 0.05$) of the XIC-derived MS spectra intensities were considered specific. Interestingly all significant proteins ($P < 0.05$) displayed a ratio ninefold or higher (Supplementary information, Table S2).

Statistical analysis

Treatment effects were analyzed in an analysis of variance procedure, and means were compared using Fisher's protected least significant difference (LSD) test ($P < 0.05$) using SAS statistical software (SAS Institute, Cary, NC, USA).

Constructs and plant transformation

Arabidopsis cDNA clones (obtained from ABRC) or amplified directly using the primers listed in Supplementary information, Table S3 were inserted into the pENTR-D/TOPO vector (Invitrogen) and verified by sequencing. The cDNAs were then transferred to pEarleyGate 101 (35S::GW-YFP) or pEarleyGate 104 (35S::YFP-GW) and introduced into *Agrobacterium tumefaciens* strain GV3101 for the transformation of *Arabidopsis* using the floral-dip method [67].

Immunocytochemistry, chemical treatments and confocal microscopy

Three-day-old seedlings were transferred for 2 h to 0.5× MS medium containing 0.8% phytoagar, to which BFA (50 μM) or ES1 (33 μM) were added.

Immunocytochemistry was carried out in *Arabidopsis* leaf protoplasts as previously described [68]. Antibodies recognizing CESA1 antibody [55], PEN1 (SYP121), Vamp72 [52] and SNAP33 [69] were diluted 1:1 000 before use. FITC-conjugated α-goat IgG and Cy3-conjugated α-rabbit IgG (Kirkegaard & Perry Laboratories) and the TRITC-conjugated α-rat IgG (Invitrogen) secondary antibodies were used at the same dilution. Samples were analyzed with TCS SP2 (Leica Microsystems), and/or LSM 510 (Carl Zeiss Microimaging) microscopes, employing sequential scanning during the colocalization experiments. Images were cropped and assembled in Adobe Photoshop CS2 for presentation purpose.

Ultrastructural analysis of isolated vesicles and Arabidopsis seedlings

Vesicles were fixed overnight at 4 °C (3% paraformaldehyde, 0.5% glutaraldehyde, 35% sucrose in 70 mM HEPES, pH 7.2), post-fixed in 2% OsO_4 and infiltrated with Spurr resin. Ultrathin sections were examined by transmission EM using a Hitachi H-7650 transmission electron microscope with a CCD camera (Hitachi High-Technologies Corporation, Japan). *Arabidopsis* samples for EM immunodetection were prepared as previously described [46].

Immunonegative staining of antibody-isolated vesicles

Immunonegative staining of the antibody-isolated vesicles was performed as described previously [70, 71] with some modification. Briefly, 10 μl of sample solution was put on carbon-coated grids and settled down in about 5 min. Excessive solution was removed using filter paper, followed by brief fixation using 1% glutaraldehyde. Grids were blocked using 3% BSA in 1× PBS

for 15 min and labeled with anti-SYP61 antibodies, followed by washing with 1% BSA. Thereafter, grids were incubated with gold-conjugated secondary antibodies for 1 h before washing with 1% BSA. Finally, grids were contrasted with 1% uranyl acetate before examination using Hitachi H-7650 transmission electron microscope with a CCD camera (Hitachi High-Technologies Corporation) operating at 80 kV.

The data associated with this manuscript may be downloaded from ProteomeCommons.org Tranche using the following hash:

ebu7tdI76xalHI7TgdB6GXyf5MuaLs7CDcOBMeP1xnMfdKBnFpVHMkHzX0XN1tGBfK/TKJSmWLrx2TAs07X2Jj9Rv3AAAAAAABKEog==

The hash may be used to prove exactly what files were published as part of this manuscript's data set, and the hash may also be used to check that the data has not changed since publication.

Acknowledgments

We thank Drs Chris Somerville (UC Berkeley, USA), Niko Geldner (University of Lausanne, Switzerland), and Herman Höfte (INRA, France) for providing the transgenic *Arabidopsis* lines CESA6-YFP, RABD2b-YFP (Wave 33), and CESA3-GFP, respectively. We also thank Drs Gerd Jürgens (University of Tuebingen, Germany), Paul Schulze-Lefert (Max Planck Institute for Plant Breeding Research, Germany), Richard Williamson (Australian National University) for providing SNAP33, PEN1 (SYP121) and SYP72 and CESA1 antibodies. We thank Drs Thomas Girke (UC Riverside, USA), Brett S Phinney (UC Davis, USA) and Mark Gjukich (University of Michigan, USA) for their support on data deposition. This work was funded by a grant from the DOE (DE-FG03-02ER15295) to NVR. GD was supported by UC Davis startup funds.

References

1 Hicks GR, Raikhel NV. Advances in dissecting endomembrane trafficking with small molecules. *Curr Opin Plant Biol* 2010; **13**:706-713.
2 Richter S, Voss U, Jurgens G. Post-Golgi traffic in plants. *Traffic* 2009; **10**:819-828.
3 Irani NG, Russinova E. Receptor endocytosis and signaling in plants. *Curr Opin Plant Biol* 2009; **12**:653-659.
4 Geldner N, Robatzek S. Plant receptors go endosomal: a moving view on signal transduction. *Plant Physiol* 2008; **147**:1565-1574.
5 Dettmer J, Hong-Hermesdorf A, Stierhof YD, Schumacher K. Vacuolar H+-ATPase activity is required for endocytic and secretory trafficking in *Arabidopsis*. *Plant Cell* 2006; **18**:715-730.
6 Viotti C, Bubeck J, Stierhof YD, *et al.* Endocytic and secretory traffic in *Arabidopsis* merge in the trans-Golgi network/early endosome, an independent and highly dynamic organelle. *Plant Cell* 2010; **22**:1344-1357.
7 Niemes S, Langhans M, Viotti C, *et al.* Retromer recycles vacuolar sorting receptors from the trans-Golgi network. *Plant J* 2010; **61**:107-121.
8 Ito J, Batth TS, Petzold CJ, *et al.* Analysis of the *Arabidopsis* cytosolic proteome highlights subcellular partitioning of central plant metabolism. *J Proteome Res* 2011; **10**:1571-1582.
9 Dunkley TP, Hester S, Shadforth IP, *et al.* Mapping the *Arabidopsis* organelle proteome. *Proc Natl Acad Sci USA* 2006; **103**:6518-6523.
10 Carter C, Pan S, Zouhar J, *et al.* The vegetative vacuole proteome of *Arabidopsis thaliana* reveals predicted and unexpected proteins. *Plant Cell* 2004; **160**:3285-3303.
11 Eubel H, Heazlewood JL, Millar AH. Isolation and subfractionation of plant mitochondria for proteomic analysis. *Methods Mol Biol* 2007; **355**:49-62.
12 Eubel H, Meyer EH, Taylor NL, *et al.* Novel proteins, putative membrane transporters, and an integrated metabolic network are revealed by quantitative proteomic analysis of *Arabidopsis* cell culture peroxisomes. *Plant Physiol* 2008; **148**:1809-1829.
13 Kleffmann T, Russenberger D, von Zychlinski A, *et al.* The *Arabidopsis thaliana* chloroplast proteome reveals pathway abundance and novel protein functions. *Curr Biol* 2004; **14**:354-362.
14 Steuble M, Gerrits B, Ludwig A, *et al.* Molecular characterization of a trafficking organelle: dissecting the axonal paths of calsyntenin-1 transport vesicles. *Proteomics* 2010; **10**:3775-3788.
15 Bassham DC, Sanderfoot AA, Kovaleva V, Zheng H, Raikhel NV. AtVPS45 complex formation at the trans-Golgi network. *Mol Biol Cell* 2000; **11**:2251-2265.
16 Sanderfoot AA, Kovaleva V, Bassham DC, Raikhel NV. Interactions between syntaxins identify at least five SNARE complexes within the Golgi/prevacuolar system of the *Arabidopsis* cell. *Mol Biol Cell* 2001; **12**:3733-3743.
17 Robert S, Chary SN, Drakakaki G, *et al.* Endosidin1 defines a compartment involved in endocytosis of the brassinosteroid receptor BRI1 and the auxin transporters PIN2 and AUX1. *Proc Natl Acad Sci USA* 2008; **105**:8464-8469.
18 Zhu JH, Gong ZZ, Zhang CQ, *et al.* OSM1/SYP61: A syntaxin protein in *Arabidopsis* controls abscisic acid-mediated and non-abscisic acid-mediated responses to abiotic stress. *Plant Cell* 2002; **14**:3009-3028.
19 Chen Y, Shin YK, Bassham DC. YKT6 is a core constituent of membrane fusion machineries at the *Arabidopsis* trans-Golgi network. *J Mol Biol* 2005; **350**:92-101.
20 Morris JA, Dorner AJ, Edwards CA, Hendershot LM, Kaufman RJ. Immunoglobulin binding protein (BiP) function is required to protect cells from endoplasmic reticulum stress but is not required for the secretion of selective proteins. *J Biol Chem* 1997; **272**:4327-4334.
21 da Silva Conceicao A, Marty-Mazars D, Bassham DC, *et al.* The syntaxin homolog AtPEP12p resides on a late post-Golgi compartment in plants. *Plant Cell* 1997; **9**:571-582.
22 Weatherly DB, Atwood JA, 3rd, Minning TA, *et al.* A Heuristic method for assigning a false-discovery rate for protein identifications from Mascot database search results. *Mol Cell Proteomics* 2005; **4**:762-772.
23 Rohila JS, Chen M, Chen S, *et al.* Protein-protein interactions of tandem affinity purified protein kinases from rice. *PLoS One* 2009; **4**:e6685.
24 Cutillas PR, Vanhaesebroeck B. Quantitative profile of five murine core proteomes using label-free functional proteomics. *Mol Cell Proteomics* 2007; **6**:1560-1573.
25 Silva JC, Denny R, Dorschel CA, *et al.* Quantitative proteom-

ic analysis by accurate mass retention time pairs. *Anal Chem* 2005; **77**:2187-2200.
26 Rojo E, Zouhar J, Kovaleva V, Hong S, Raikhel NV. The AtC-VPS protein complex is localized to the tonoplast and the prevacuolar compartment in *Arabidopsis*. *Mol Biol Cell* 2003; **14**:361-369.
27 Paredez AR, Somerville CR, Ehrhardt DW. Visualization of cellulose synthase demonstrates functional association with microtubules. *Science* 2006; **312**:1491-1495.
28 Whiteheart SW, Griff IC, Brunner M, *et al.* SNAP family of NSF attachment proteins includes a brain-specific isoform. *Nature* 1993; **362**:353-355.
29 Zouhar J, Munoz A, Rojo E. Functional specialization within the Vacuolar Sorting Receptor family: VSR1, VSR3 and VSR4 sort vacuolar storage cargo in seeds and vegetative tissues. *Plant J* 2010; **64**:577-588.
30 Yang X, Matern HT, Gallwitz D. Specific binding to a novel and essential Golgi membrane protein (Yip1p) functionally links the transport GTPases Ypt1p and Ypt31p. *EMBO J* 1998; **17**:4954-4963.
31 Tang BL, Ong YS, Huang B, *et al*. A membrane protein enriched in endoplasmic reticulum exit sites interacts with COPII. *J Biol Chem* 2001; **276**:40008-40017.
32 Kano F, Yamauchi S, Yoshida Y, *et al.* Yip1A regulates the COPI-independent retrograde transport from the Golgi complex to the ER. *J Cell Sci* 2009; **122**:2218-2227.
33 Geldner N, Denervaud-Tendon V, Hyman DL, *et al.* Rapid, combinatorial analysis of membrane compartments in intact plants with a multicolor marker set. *Plant J* 2009; **59**:169-178.
34 Pinheiro H, Samalova M, Geldner N, *et al.* Genetic evidence that the higher plant Rab-D1 and Rab-D2 GTPases exhibit distinct but overlapping interactions in the early secretory pathway. *J Cell Sci* 2009; **122**:3749-3758.
35 Markgraf DF, Peplowska K, Ungermann C. Rab cascades and tethering factors in the endomembrane system. *FEBS Lett* 2007; **581**:2125-2130.
36 Sztul E, Lupashin V. Role of tethering factors in secretory membrane traffic. *Am J Physiol Cell Physiol* 2006; **290**:C11-26.
37 Thellmann M, Rybak K, Thiele K, Wanner G, Assaad FF. Tethering factors required for cytokinesis in *Arabidopsis*. *Plant Physiol* 2010; **154**:720-732.
38 Wang W, Sacher M, Ferro-Novick S. TRAPP stimulates guanine nucleotide exchange on Ypt1p. *J Cell Biol* 2000; **151**:289-296.
39 Holwerda BC, Padgett HS, Rogers JC. Proaleurain vacuolar targeting is mediated by short contiguous peptide interactions. *Plant Cell* 1992; **4**:307-318.
40 Bednarek SY, Wilkins TA, Dombrowski JE, Raikhel NV. A carboxyl-terminal propeptide is necessary for proper sorting of barley lectin to vacuoles of tobacco. *Plant Cell* 1990; **2**:1145-1155.
41 Shimada T, Fuji K, Tamura K, *et al.* Vacuolar sorting receptor for seed storage proteins in *Arabidopsis thaliana*. *Proc Natl Acad Sci USA* 2003; **100**:16095-16100.
42 Avila EL, Brown M, Pan S, *et al.* Expression analysis of *Arabidopsis* vacuolar sorting receptor 3 reveals a putative function in guard cells. *J Exp Bot* 2008; **59**:1149-1161.
43 Ahmed SU, Bar-Peled M, Raikhel NV. Cloning and subcellular location of an *Arabidopsis* receptor-like protein that shares common features with protein-sorting receptors of eukaryotic cells. *Plant Physiol* 1997; **114**:325-336.
44 Hinz G, Colanesi S, Hillmer S, Rogers JC, Robinson DG. Localization of vacuolar transport receptors and cargo proteins in the Golgi apparatus of developing *Arabidopsis* embryos. *Traffic* 2007; **8**:1452-1464.
45 Otegui MS, Herder R, Schulze J, Jung R, Staehelin LA. The proteolytic processing of seed storage proteins in *Arabidopsis* embryo cells starts in the multivesicular bodies. *Plant Cell* 2006; **18**:2567-2581.
46 Miao Y, Yan PK, Kim H, Hwang I, Jiang L. Localization of green fluorescent protein fusions with the seven *Arabidopsis* vacuolar sorting receptors to prevacuolar compartments in tobacco BY-2 cells. *Plant Physiol* 2006; **142**:945-962.
47 Niemes S, Langhans M, Viotti C, *et al.* Retromer recycles vacuolar sorting receptors from the trans-Golgi network. *Plant J* 2010; **61**:107-121.
48 Foresti O, Gershlick DC, Bottanelli F, *et al.* A recycling-defective vacuolar sorting receptor reveals an intermediate compartment situated between prevacuoles and vacuoles in tobacco. *Plant Cell* 2010; **22**:3992-4008.
49 Saint-Jean B, Seveno-Carpentier E, Alcon C, Neuhaus JM, Paris N. The cytosolic tail dipeptide Ile-Met of the pea receptor BP80 is required for recycling from the prevacuole and for endocytosis. *Plant Cell* 2010; **22**:2825-2837.
50 Fasshauer D, Sutton RB, Brunger AT, Jahn R. Conserved structural features of the synaptic fusion complex: SNARE proteins reclassified as Q- and R-SNAREs. *Proc Natl Acad Sci USA* 1998; **95**:15781-15786.
51 Collins NC, Thordal-Christensen H, Lipka V, *et al.* SNARE-protein-mediated disease resistance at the plant cell wall. *Nature* 2003; **425**:973-977.
52 Kwon C, Neu C, Pajonk S, *et al.* Co-option of a default secretory pathway for plant immune responses. *Nature* 2008; **451**:835-840.
53 Kwaaitaal M, Keinath NF, Pajonk S, Biskup C, Panstruga R. Combined bimolecular fluorescence complementation and Forster resonance energy transfer reveals ternary SNARE complex formation in living plant cells. *Plant Physiol* 2010; **152**:1135-1147.
54 Leyman B, Geelen D, Quintero FJ, Blatt MR. A tobacco syntaxin with a role in hormonal control of guard cell ion channels. *Science* 1999; **283**:537-540.
55 Wang J, Elliott JE, Williamson RE. Features of the primary wall CESA complex in wild type and cellulose-deficient mutants of *Arabidopsis thaliana*. *J Exp Bot* 2008; **59**:2627-2637.
56 Crowell EF, Bischoff V, Desprez T, *et al.* Pausing of Golgi bodies on microtubules regulates secretion of cellulose synthase complexes in *Arabidopsis*. *Plant Cell* 2009; **21**:1141-1154.
57 Gutierrez R, Lindeboom JJ, Paredez AR, Emons AM, Ehrhardt DW. *Arabidopsis* cortical microtubules position cellulose synthase delivery to the plasma membrane and interact with cellulose synthase trafficking compartments. *Nat Cell Biol* 2009; **11**:797-806.
58 Toyooka K, Goto Y, Asatsuma S, *et al.* A mobile secretory vesicle cluster involved in mass transport from the Golgi to

the plant cell exterior. *Plant Cell* 2009; **21**:1212-1229.
59 Lam SK, Siu CL, Hillmer S, *et al*. Rice SCAMP1 defines clathrin-coated, trans-golgi-located tubular-vesicular structures as an early endosome in tobacco BY-2 cells. *Plant Cell* 2007; **19**:296-319.
60 Gendre D, Oh J, Boutte Y, *et al*. Conserved *Arabidopsis* ECHIDNA protein mediates trans-Golgi-network trafficking and cell elongation. *Proc Natl Acad Sci USA* 2011; **108**:8048-8053.
61 Robinson DG, Jiang LW, Schumacher K. The endosomal system of plants: Charting new and familiar territories. *Plant Physiol* 2008; **147**:1482-1492.
62 Inadome H, Noda Y, Kamimura Y, Adachi H, Yoda K. Tvp38, Tvp23, Tvp18 and Tvp15: novel membrane proteins in the Tlg2-containing Golgi/endosome compartments of Saccharomyces cerevisiae. *Exp Cell Res* 2007; **313**:688-697.
63 Kang BH, Nielsen E, Preuss ML, Mastronarde D, Staehelin LA. Electron tomography of RabA4b- and PI-4Kbeta1-Labeled trans golgi network compartments in *Arabidopsis*. *Traffic* 2010; **12**:313-329.
64 Zabotina OA, van de Ven WT, Freshour G, *et al. Arabidopsis* XXT5 gene encodes a putative alpha-1,6-xylosyltransferase that is involved in xyloglucan biosynthesis. *Plant J* 2008; **56**:101-115.
65 Drakakaki G, Zabotina O, Delgado I, *et al. Arabidopsis* reversibly glycosylated polypeptides 1 and 2 are essential for pollen development. *Plant Physiol* 2006; **142**:1480-1492.
66 Voisin SN, Krakovska O, Matta A, *et al.* Identification of novel molecular targets for endometrial cancer using a drill-down LC-MS/MS approach with iTRAQ. *PLoS One* 2011; **6**:e16352.
67 Clough SJ, Bent AF. Floral dip: a simplified method for *Agrobacterium*-mediated transformation of *Arabidopsis thaliana*. *Plant J* 1998; **16**:735-743.
68 Sohn EJ, Rojas-Pierce M, Pan S, *et al.* The shoot meristem identity gene TFL1 is involved in flower development and trafficking to the protein storage vacuole. *Proc Natl Acad Sci USA* 2007; **104**:18801-18806.
69 Heese M, Gansel X, Sticher L, *et al.* Functional characterization of the KNOLLE-interacting t-SNARE AtSNAP33 and its role in plant cytokinesis. *J Cell Biol* 2001; **155**:239-249.
70 Tse YC, Mo B, Hillmer S, *et al.* Identification of multivesicular bodies as prevacuolar compartments in *Nicotiana tabacum* BY-2 cells. *Plant Cell* 2004; **16**:672-693.
71 Wang J, Li Y, Lo SW, *et al.* Protein mobilization in germinating mung bean seeds involves vacuolar sorting receptors and multivesicular bodies. *Plant Physiol 2007*; **143**:1628-1639.

(**Supplementary Information** is linked to the online version of the paper on the *Cell Research* website.)